# QUANTIFICATION OF LONG PERIOD STRONG GROUND MOTION ATTENUATION FOR ENGINEERING DESIGN

W. Silva and N. A. Abrahamson

Pacific Engineering and Analysis, El Cerrito, CA 94530

## ABSTRACT

Empirical strong motion recordings from large magnitude (M≥6) events are reprocessed with an emphasis toward preserving the long period motions. A preliminary empirical attenuation relationship for response spectral values is derived for the period range 1-20 seconds.

## INTRODUCTION

The major difficulty in estimating long period spectral attenuation relations from empirical data is that much of the processed data are near or below the noise level at periods greater than several seconds. To address this problem, we have reprocessed the recordings from large magnitude events using a procedure that is directed at recovering the long period motion. In addition, we have applied a new procedure for evaluating the noise level for long period motions.

Based on our analysis, at periods greater than 10 seconds, very few of the accelerograms contain energy above the noise level. We used numerical modeling to guide the extension of the attenuation relations to periods up to 20 seconds.

This paper describes the preliminary long period attenuation relations derived using recordings from the larger magnitude events. The final attenuation relations will include a larger set of data.

## DATA BASE

The events used in the initial analysis are listed in Table 1. Based upon site response analyses using provincial categories and generic site profiles (Silva, 1991) the sites were initially classified as rock, shallow soil (<250 ft), intermediate depth soil (250-1000 ft), deep soil (>1000 ft), and alluvium of unknown depth. There are insufficient recordings in the shallow and intermediate categories to evaluate these categories separately. Therefore, we combined the data into two groups: soil < 250 ft and soil > 250 ft. The "alluvium of unknown depth" was put into the soil > 250 ft group. The distribution of recordings in magnitude and distance is shown in Figure 1. Distance is defined as closest distance to the seismogenic zone (Campbell, 1991) and magnitude is moment magnitude.

## CORRECTION PROCEDURE

In order to extend the strong motion data base to as long of periods as possible, all records were reprocessed. The correction procedure used involves a series of five steps: 1) interpolation of uncorrected unevenly sampled records to 400 samples/sec, 2) frequency domain low-pass filtering using a causal 5-pole Buterworth filter with corner frequencies selected for each record based upon visual examination of the Fourier amplitude spectrum, 3) removing the instrument response, 4) decimating to 100 or 200 samples/sec depending upon the low-pass filter corner frequencies, and 5) applying a time domain baseline correction procedure and a final high-pass

filter. The baseline correction procedure uses polynomials in degree from 0-10 depending upon initial integrated displacements. The characteristic of the high-pass filter is that of an overdamped oscillator (Grazer, 1979). It is flat about its corner frequency and falls off proportional to frequency on either side. The filter is applied in the time domain twice, forward and reverse, resulting in a zero phase shift processed record. As with the polynomial baseline correction, the high-pass filter parameters are based upon visual examination of the filtered integrated displacements for a suite of parameter values. The response spectral values are only used in the regression if the frequency is greater than 1.25 times the high-pass filter corner frequency. This insures that the filter will not have a significant effect on the spectral values.

The visual examination of the displacements and the judgment as to the appropriate filter is based on the consistency of the amplitudes and timing of the long period energy with that of the higher frequency motion. One way to quantify the consistency of the timing of the long period motions is by examining the phase spectrum. The phase spectrum controls the timing and shape of the waveform. Seismic ground motion are expected to have a consistent phase structure at long periods whereas noise will have random phase.

Specifically, we examine the analytical derivative of the phase with respect to frequency (Tribolet, 1977). Examples of the phase derivative are shown in Figures 2a and b. Figure 2a shows a case where the phase derivative is well behaved to periods of 20 seconds. In contrast, Figure 2b shows a case where the phase derivative becomes much more random at a period of about 1.5 seconds. The final corrected acceleration time histories are evaluated for long period noise contamination by examining the analytic phase derivative. Response spectra values are only used in the regression analyses for periods at which the phase derivatives are well behaved.

## REGRESSION ANALYSES

The regression analyses use the random effects model following the algorithm of Abrahamson and Youngs (1992). The random effects model explicitly models the correlation between recordings from the same earthquake. It handles uneven sampling of the earthquakes in a statistically optimal manner. This method partitions the variance into inter-event ($\tau^2$) and intra-event ($\sigma^2$) terms.

The regression is performed for peak acceleration (pga) and response spectral values. The regression for response spectral values uses the normalized spectral shape (Sa/pga) because the data set is too small to allow stable regression on the absolute spectral values. The final response spectral attenuation is found by combining the spectra shape model with the pga model.

The peak acceleration is modeled by the following functional form:

$$\ln \text{pga(g)} = c_1 + c_2 M + c_3 \ln(r+20) + c_4 F \qquad (1)$$

where r is the distance in km and F is the fault type (F=0 for SS, and F=1 for reverse or oblique). Because the subset of the data used in this preliminary analysis has a limited range of magnitudes, the magnitude dependence is not well constrained by the data. Similarly, for the small number of events, the fault type dependence is also not well constrained. Therefore, the $c_2$ and $c_4$ parameters were fixed based on previous studies of larger data sets: $c_2$=1.2, $c_4$=0.25 (Campbell, 1991; PG&E, 1990).

The estimated coefficients for pga are listed in Table 2. The residuals are plotted in Figure 3. The residuals show a slight increase at distances of 70 to 100 km. To test if the attenuation is flat over this range (as the result of the Moho bounce), the regression was repeated using a flat attenuation from 70 to 90 km. The resulting solution produced a smaller likelihood than the

initial solution without flattening. This data set does not support a significant flattening of the pga attenuation for distances less than 100 km.

The functional form for the spectral shape was guided by results from numerical simulations and previous empirical studies. Depending on the assumptions regarding the seismic source parameter values, simulations suggest that strike-slip events maybe more likely to show near-field directivity effects at long periods than reverse events . The functional form is selected so that it can accommodate this effect. The normalized spectrum is model by

$$\ln\left(\frac{Sa}{pga}\right) = c_1 + c_3 r + c_4(1-\tanh\{(r^{1.1} - 10)/3\})(1-F) \qquad (2)$$

The last term accommodates the near-field effect for strike-slip events. As with the pga, the magnitude dependence of the spectral shape cannot be reliably determined from this data set. Therefore, the magnitude dependence is not modeled in this preliminary regression.

The coefficients computed for the rock/shallow soil and deep soil site conditions are listed in Table 3. The near-field term, $c_4$, corresponds to a 35% difference in long period spectral shape at short distances. The empirical data could only be used for periods up to 7.5 seconds because there were not enough records with reliable long periods to justify a high-pass corner frequency lower than 0.1 Hz. Based on numerical simulations, the response spectrum is approximately flat to spectral displacement at periods greater than 8 seconds for magnitudes less than 7.5. The spectral attenuation relations were extended to 20 seconds assuming constant spectral displacement. For magnitudes larger than 7.5, this extension my not be appropriate.

This data set shows a strong distance dependence of the spectral shape. This effect is dominated by the recordings from the Loma Prieta earthquake. The Loma Prieta Earthquake is a major portion of the data set and the distance dependence of the spectral shape may be reduced when the full data set is used.

The spectral attenuation relation for a magnitude 7.0 strike-slip event at deep soil and rock/shallow soil sites are shown in Figures 4a and 4b, respectively. In Figure 5a and 5b, the deep soil attenuation relation is compared to the Joyner and Boore (1982) and Sadigh (1987) attenuation relations for soil for distances of 10 and 50 km. The attenuation relation from this study is significantly lower than the Sadigh and Joyner and Boore relations at 10 km, but it is similar at 50 km. This is due to the strong distance dependence of the spectral shape discussed earlier. A similar comparison for the rock/shallow soil site model is shown in Figures 6a and 6b.

## REFERENCES

Abrahamson, N.A. and R.P. Youngs (1992). A stable algorithm for regression analyses using the random effects model, Bull. Seism. Soc. Am., 505-510.

Campbell, K. W. (1991). A random-effects analysis of near-source ground motion for the Diablo Canyon Power Plant site, San Luis Obispo County, California, Report prepared for LLNL.

Grazier, V. M. (1979). Determination of the true ground displacement by using strong motion records, Phys. Solid Earth, Izv. Acad. Sc. USSR. English edition published by Am. Geophys. Union, 15:(12) 875-885.

Joyner, W. B. and D. M. Boore (1982). Prediction of earthquake response spectra, U.S. Geol.Surv. OFR 82-977.

PG&E (1990). Response to workshop question 4, NRC Docket Nos. 50-275 and 50-323, August 1990.

Silva, W. (1991). Site geometry and global characteristics, Proc. NSF/EPRI Workshop on Dynamic Soil Properties and Site Characterization, Palo Alto, CA.

Tribolet, S.M. (1977). A new phase unwrapping algorithm, IEEE Trans, ASSP-25, 170-177.

Table 1. List of Earthquakes Used in Preliminary Analysis

| Event | Mw | R | S | I | D | A | Total |
|---|---|---|---|---|---|---|---|
| 1940 El Centro | 7.0 | | | | 1 | | 1 |
| 1952 Kern County | 7.4 | | | | 3 | 1 | 4 |
| 1966 Parkfield | 6.1 | 2 | | | 4 | | 6 |
| 1968 Borrego Mtn. | 6.6 | | | | 1 | | 1 |
| 1971 San Fernando | 6.6 | 11 | 1 | 1 | 6 | 1 | 20 |
| 1976 Gazli | 6.8 | | | | 1 | | 1 |
| 1978 Tabas | 7.4 | | | | 2 | | 2 |
| 1979 Imperial Valley | 6.5 | | | | 19 | | 19 |
| 1983 Coalinga | 6.5 | 21 | | | 1 | 3 | 25 |
| 1985 Nahanni | 6.8 | 3 | | | | | 3 |
| 1988 Spitak | 7.0 | 1 | | | | | 1 |
| 1989 Loma Prieta | 7.0 | 28 | 5 | 2 | 13 | 5 | 53 |
| Total | | 66 | 6 | 3 | 51 | 10 | 136 |

R=rock, S=shallow soil, I=intermediate depth soil, D=deep soil, A=alluvium of unknown depth.

Table 2. Estimated Coefficients for PGA Model for the Average Horizontal Component

| Coeff | Deep Soil | Rock/Shallow Soil |
|---|---|---|
| $c_1$ | -3.27 | -3.56 |
| $c_2$ | 1.2 | 1.2 |
| $c_3$ | -1.79 | -1.67 |
| $c_4$ | 0.25 | 0.25 |
| $\sigma_{Total}$ | 0.46 | 0.46 |

Table 3. Estimated Coefficients for Spectral Shape for the Average Horizontal Component

| Period | Deep Soil $c_1$ | Rock $c_1$ | $c_3$ | $c_4$ | $\sigma_{Total}$ | $\sigma$ | $\tau$ |
|---|---|---|---|---|---|---|---|
| 1.0 | -0.224 | -0.525 | 0.011 | 0.15 | 0.54 | 0.45 | 0.30 |
| 1.5 | -0.587 | -1.056 | 0.010 | 0.15 | 0.57 | 0.49 | 0.28 |
| 2.0 | -0.965 | -1.380 | 0.010 | 0.15 | 0.59 | 0.55 | 0.23 |
| 3.0 | -1.453 | -1.861 | 0.008 | 0.15 | 0.63 | 0.62 | 0.13 |
| 4.0 | -1.920 | -2.315 | 0.008 | 0.15 | 0.62 | 0.60 | 0.18 |
| 5.0 | -2.009 | -2.565 | 0.007 | 0.15 | 0.67 | 0.67 | 0.00 |
| 7.7 | -2.965 | -3.442 | 0.014 | 0.15 | 0.80 | 0.80 | 0.00 |
| 10.0 | -3.49 | -3.96 | 0.014 | 0.15 | 0.80 | 0.80 | 0.00 |
| 15.0 | -4.30 | -4.78 | 0.014 | 0.15 | 0.80 | 0.80 | 0.00 |
| 20.0 | -4.87 | -5.35 | 0.014 | 0.15 | 0.80 | 0.80 | 0.00 |

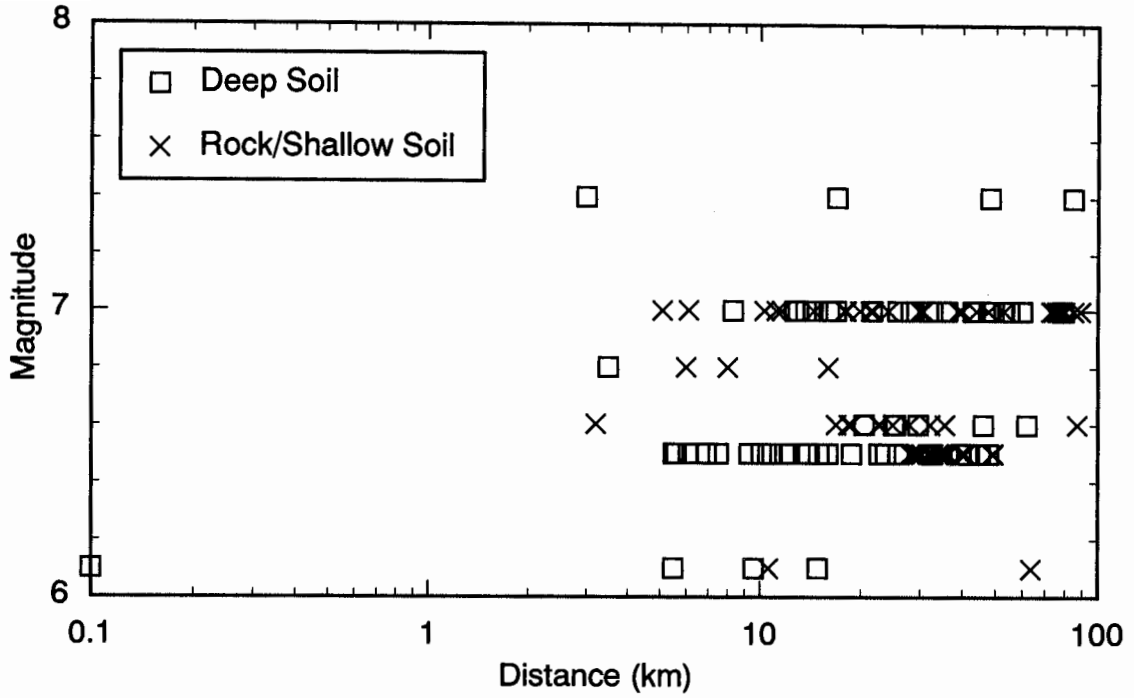


Figure 1. Data set used in the preliminary analysis.

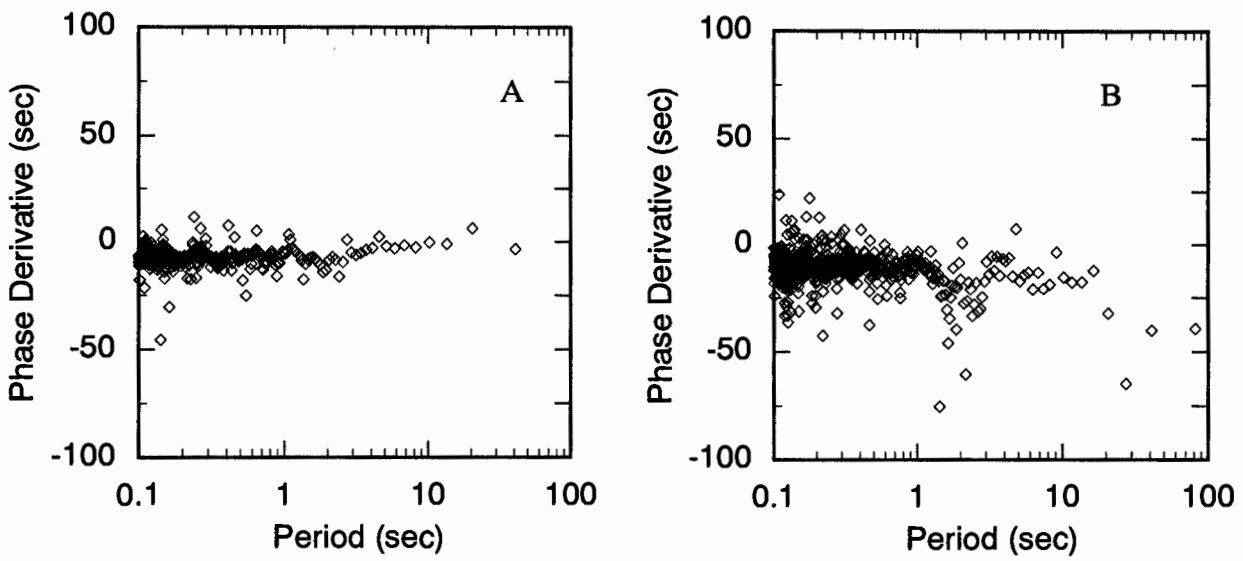


Figure 2. Sample analytical phase derivatives. Panel A shows a case in which the phase derivative is well behaved for periods up to 30 seconds. Panel B shows a case in which the phase derivative becomes more random at a period of about 1.5 seconds.

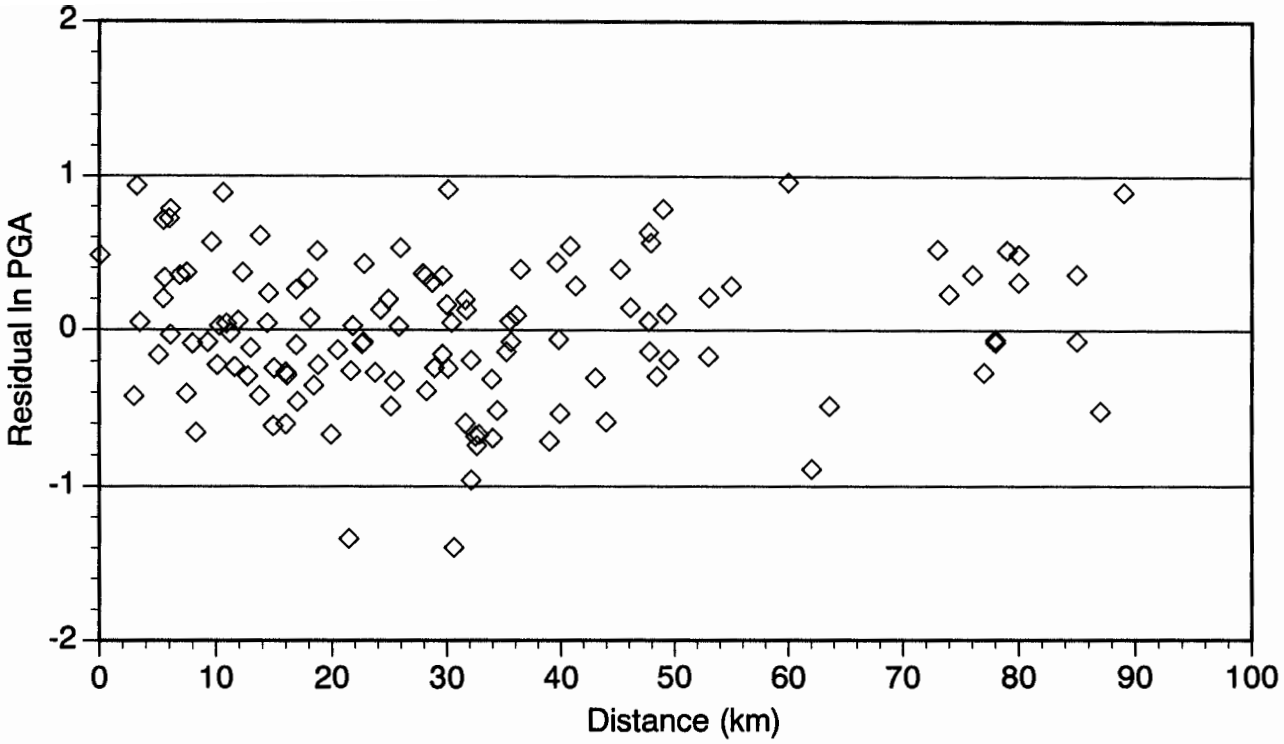


Figure 3. Peak acceleration residuals (intra-event) from Eq. 1. The residuals do not indicate that there is a significnat flattening in the attenuation for distances less than 100 km.

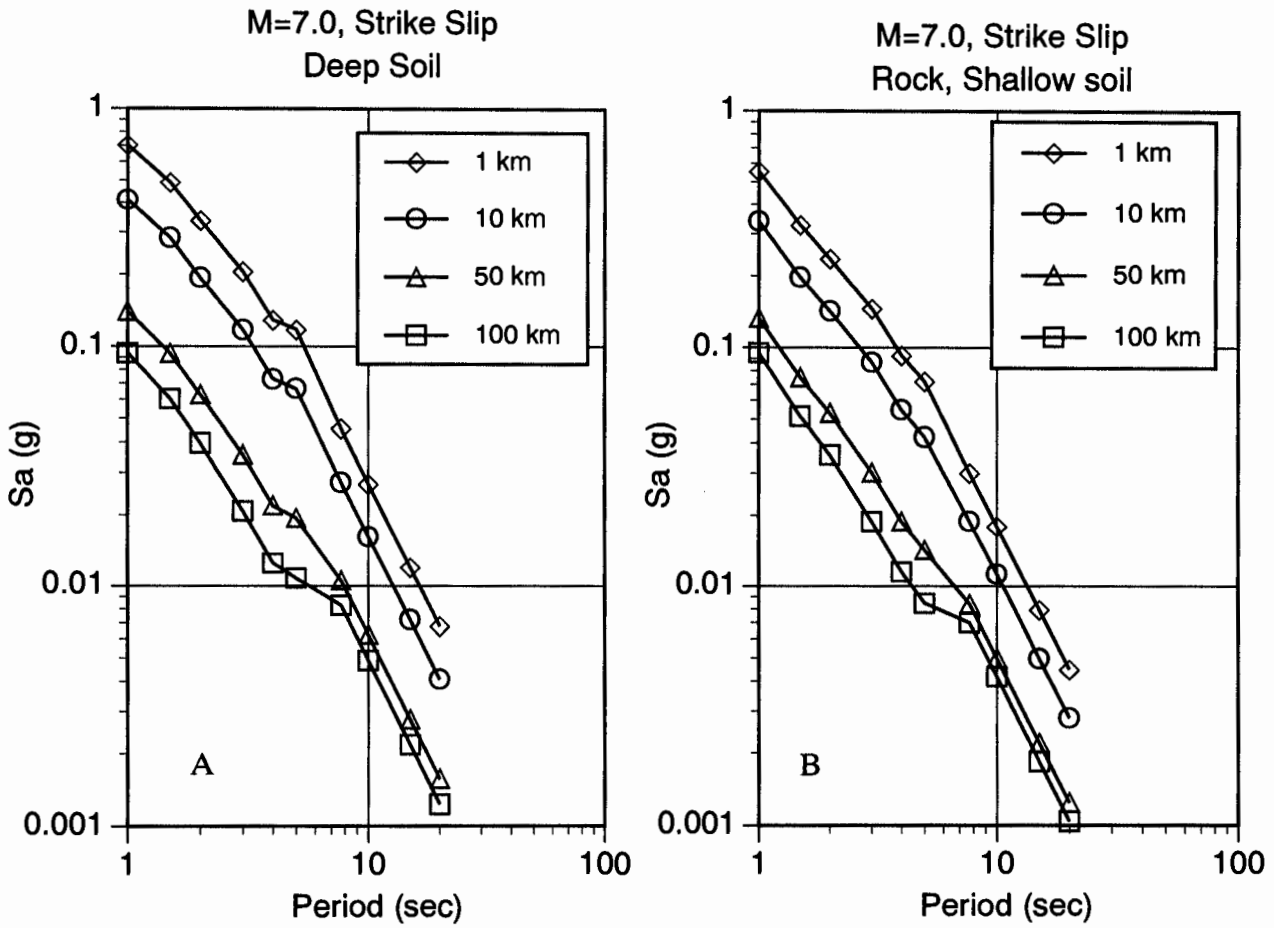


Figure 4. Attenuation of Long period spectral acceleration from Eq. 2 for a magnitude 7.0 strike-slip event. The coefficients are not smoothed. (A) Deep soil sites. (B) Rock / shallow soil sites.

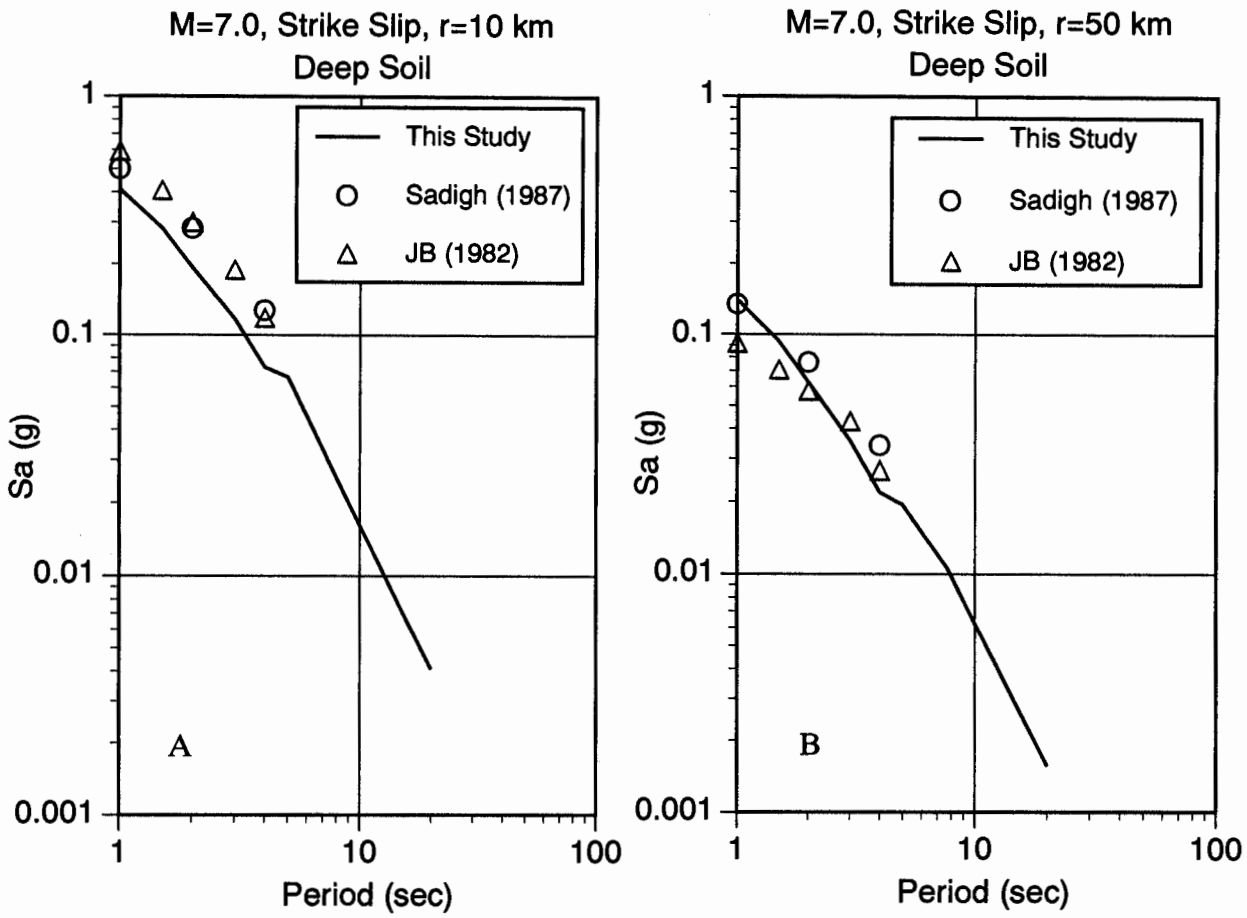


Figure 5. Comparison of the long period spectral acceleration from Eq. 2 for a magnitude 7.0 strike-slip event at deep soil sites with previously published empirical models. The relation from this study shows a much strong distance dependent spectral shape which accounts for the large differences seen in panel A. Since the distance dependence is dominated by the Loma Prieta earthquake, it is expected to be reduced when the larger data set is analyzed.

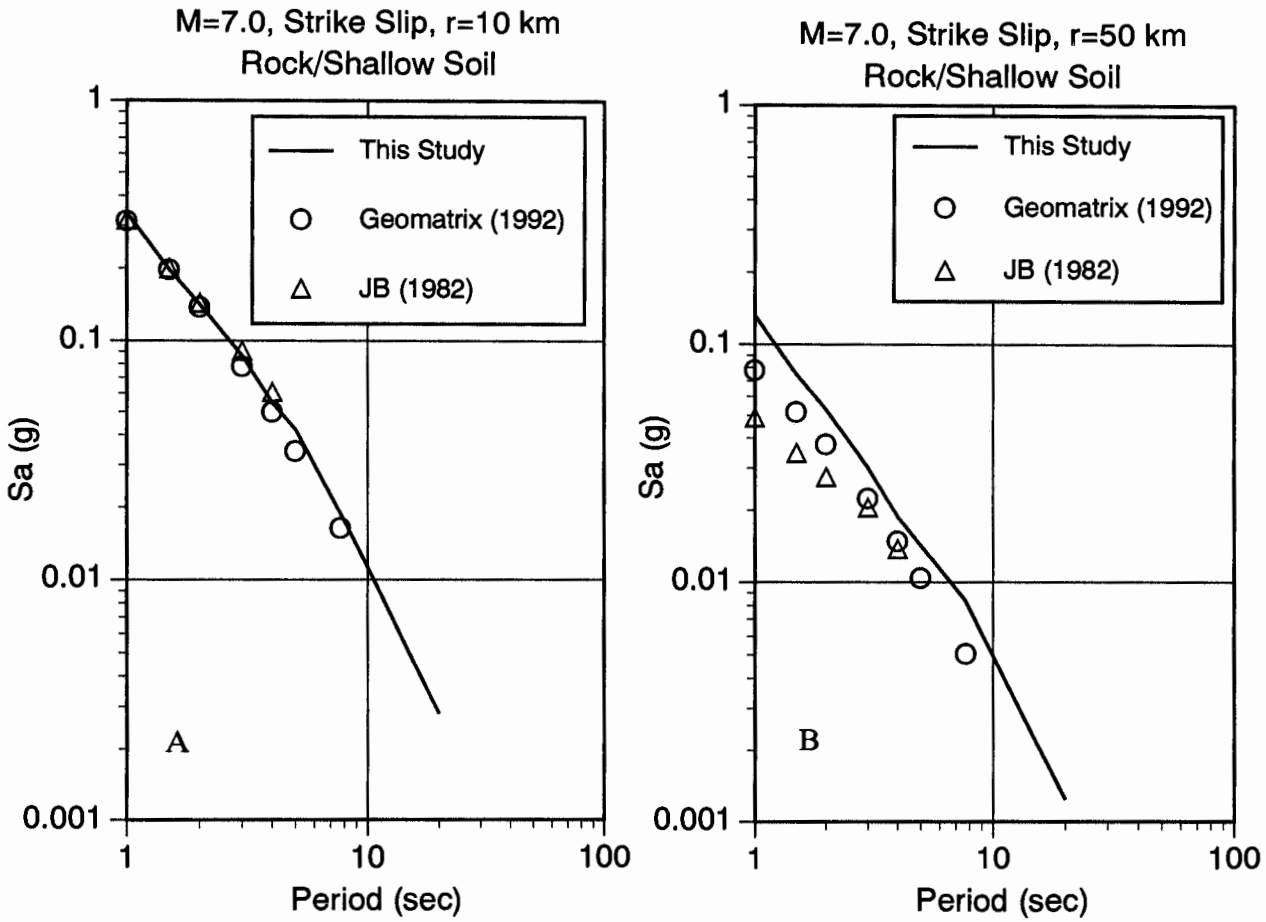


Figure 6. Comparison of the long period spectral acceleration from Eq. 2 for a magnitude 7.0 strike-slip event at rock/shallow soil sites with previously published empirical models for rock. As in Figure 5, the relation from this study shows a much strong distance dependent spectral shape which accounts for the large differences seen in panel B.

# SMIP92 Seminar Proceedings